ELSEVIER

Journal of Hydrology 222 (1999) 109–122

Journal of Hydrology

Groundwater flow near vertical recirculatory wells: effect of skin on flowgeometry and travel times with implications for aquifer remediation

D.V. Peursem[a,*], V. Zlotnik[b], G. Ledder[c]

[a]*Department of Mathematical Sciences, University of South Dakota, Vermillion, SD 57069-2390, USA*
[b]*Department of Geosciences, University of Nebraska, Lincoln, NE 68588-0340, USA*
[c]*Department of Mathematics and Statistics, University of Nebraska, Lincoln, NE 68588-0323, USA*

Received 22 December 1998; accepted 1 July 1999

Abstract

Flow structure around a recirculation well in a uniform anisotropic aquifer is investigated using potential theory and Stokes' stream function techniques. A vertical recirculation well consists of two screened sections (chambers) separated by an impermeable casing: one section extracts water from the aquifer and the other section injects the water back into the aquifer. Analytical formulae are derived for the drawdown and the stream function for a model in which the extraction and injection chambers of the well are modeled as uniformly distributed cylindrical sinks and sources, respectively. Travel times are analyzed for water particles traveling from the injection chamber to the extraction chamber along streamlines containing various percentages of the flow. We consider a disturbed zone (skin) having properties which are different from those in the uniform anisotropic aquifer owing to disturbance of the area near the well during installation. The effects of this skin on the streamlines and travel times are analyzed for various lengths separating the chambers and for various skin conductivities. The method completely eliminates the use of numerical finite-difference or finite-element methods and can be used for optimization of technological parameters in a remediation system.

Keywords: Vertical recirculation; Well; Skin; Streamlines; Travel times; Saturated flow

1. Introduction

Herrling and Buermann (1990), Herrling et al. (1991) and Herrling and Stamm (1992) proposed an aquifer remediation technique that has received significant attention in literature and in practice. This method employs a vertical circulation well consisting of two screened sections (chambers) that are separated by an impermeable casing (Fig. 1). After a short time, a steady vertical circulation flow is achieved. Water is extracted from the aquifer through one chamber and injected into the aquifer through the other with equal flow rates, removing contaminants at the surface or introducing various chemical agents for remediation into the groundwater. Some modifications of this system were proposed by Gvirtzman and Gorelick (1992, 1993).

Another possible application for recirculation systems is the estimation of aquifer properties such as the radial hydraulic conductivity and the anisotropy ratio. Some work has already been done on this application by Kabala (1993), Zlotnik and Ledder (1994,

* Corresponding author. Fax: + 1-605-677-5263.
E-mail addresses: dpeursem@usd.edu (D.V. Peursem), vzlotnik@unlinfo.unl.edu (V. Zlotnik), gledder@math.unl.edu (G. Ledder)

0022-1694/99/$ - see front matter
PII: S0022-1694(99)00100-6

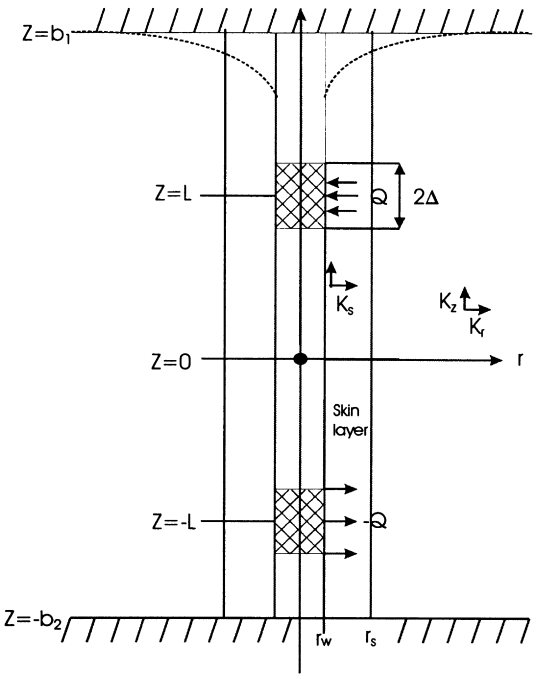

Fig. 1. Schematic diagram of a vertical circulation well (dipole) with a skin layer.

1996), Indelman and Zlotnik (1997) and Zlotnik and Zurbuchen (1998).

It has been demonstrated by Zlotnik and Ledder (1996) and Van Peursem et al. (1998), that potential theory and Stokes' stream function techniques are efficient tools to reduce computer-intensive finite-difference (Gvirtzman and Gorelick, 1992, 1993), or finite-element (Herrling and Stamm, 1992) calculations of the drawdown and flow paths.

Zlotnik and Ledder (1996) and Van Peursem et al. (1998) determined drawdown and streamlines for a vertical circulation well in a uniform anisotropic aquifer by modeling the well as a uniformly distributed line source and sink. However, one concern is that a skin layer caused by the disturbed region near the well during drilling may cause a "short-circuiting" in the particle path between well chambers due to a higher conductivity of back fill material (Kabala and Xiang, 1992). If such a short-circuiting should occur, the flow lines would be deformed and therefore not have as great a region of influence, thereby reducing the efficiency of aquifer remediation or the accuracy of parameter estimation.

The purpose of this paper is to study the effects of the skin on the streamlines and travel times as well as other factors that may enhance the effects of the skin such as boundaries, anisotropy, and various aspect ratios.

2. Head distribution

2.1. General problem statement

We first consider the problem for the steady-state drawdown of a vertical recirculation well in a homogeneous anisotropic aquifer of infinite extent. The method of images is then used to determine solutions for confined aquifers of infinite and finite thickness. However, Zlotnik and Ledder (1994) have shown that the infinite model can be used whenever the aquifer boundaries are at least $2L$ from the center of the vertical circulation well, where L is half of the distance between the centers of the screened sections. Let $z = 0$ be the center of the screened sections, $r = 0$ be the center of the well, $r = r_w$ be the well radius where the sinks and sources along the screened sections of the well are assumed to be distributed uniformly, and Δ be half the length of each screened section (Fig. 1). It is assumed that the skin layer is uniform and isotropic, with constant conductivity K_s, and the aquifer is uniform and anisotropic, having constant vertical and radial hydraulic conductivities of K_z and K_r, respectively.

The drawdown in hydraulic head inside the skin s_1 and outside the skin s_2 are determined separately, and then the two solutions are matched by forcing continuity in the drawdown and flux at $r = r_s$. The governing equations are

$$\frac{K_s}{r}\frac{\partial}{\partial r}\left(r\frac{\partial s_1}{\partial r}\right) + K_s\frac{\partial^2 s_1}{\partial z^2} = 0, \qquad 0 < r < r_s, \quad -\infty < z < \infty, \tag{1}$$

$$\frac{K_r}{r}\frac{\partial}{\partial r}\left(r\frac{\partial s_2}{\partial r}\right) + K_z\frac{\partial^2 s_2}{\partial z^2} = 0, \qquad r_s < r < \infty, \quad -\infty < z < \infty, \tag{2}$$

$$\lim_{r\to r_w} r\frac{\partial s_1}{\partial r}(r,z) = \frac{QF(z)}{4\pi\Delta K_s}, \qquad -\infty < z < \infty, \tag{3}$$

where

$$F(z) = \begin{cases} -1, & \text{if } |z - L| < \Delta \\ 1, & \text{if } |z + L| < \Delta \\ 0, & \text{otherwise} \end{cases} \quad (4)$$

$$s_2(\infty, z) = 0, \qquad -\infty < z < \infty, \quad (5)$$

$$s_1(r_s, z) = s_2(r_s, z), \qquad -\infty < z < \infty, \quad (6)$$

$$K_s \frac{\partial s_1}{\partial r}(r_s, z) = K_r \frac{\partial s_2}{\partial r}(r_s, z), \qquad -\infty < z < \infty, \quad (7)$$

$$K_s \frac{\partial s_1}{\partial z}(r, -\infty) = K_s \frac{\partial s_1}{\partial z}(r, \infty) = 0, \qquad r_w < r < r_s, \quad (8)$$

$$K_z \frac{\partial s_2}{\partial z}(r, -\infty) = K_z \frac{\partial s_2}{\partial z}(r, \infty) = 0, \qquad r_s < r < \infty. \quad (9)$$

The only difference in the problem statement for a finite aquifer is that in Eqs. (1)–(7), the vertical domain of interest is $-b_2 < z < b_1$, and the boundary conditions in Eqs. (8) and (9) are applied at $z = -b_2$ and $z = b_1$.

2.2. Drawdown solution inside the skin for an aquifer of infinite thickness

The drawdown inside of the skin region is derived in Appendix A and given by

$$s_1(r, z) = \frac{-iQ}{4\pi^2 \Delta K_s r_w} \int_0^\infty J(\xi)[g(\xi) I_0(r\xi) + K_0(r\xi)] \sin(\xi z)\, d\xi, \quad (10)$$

$$r_w < r < r_s,$$

$$J(\xi) = \frac{\hat{F}(\xi)}{|\xi|[g(\xi) I_1(r_w\xi) - K_1(r_w\xi)]}, \quad (11)$$

$$\hat{F}(\xi) = -\frac{4i \sin(\xi L) \sin(\xi \Delta)}{\xi}, \quad (12)$$

$$g(\xi) = \frac{cK_1(r_s|\xi|)K_0(r_s|\xi|/a) - K_0(r_s|\xi|)K_1(r_s|\xi|/a)}{cI_1(r_s|\xi|)K_0(r_s|\xi|/a) + I_0(r_s|\xi|)K_1(r_s|\xi|/a)}, \quad (13)$$

$$c = \frac{K_s a}{K_r} = \frac{K_s}{\sqrt{K_r K_z}}, \quad (14)$$

and $a^2 = K_r/K_z$. The functions, K_0, K_1, I_0 and I_1, are modified Bessel functions. Note that s_1 is odd in z, as expected from the geometry of the problem. We also note that in the no-skin case ($a = c = 1$ and $g(\xi) = 0$) with $r_w = 0$, this solution reduces to the solution of Zlotnik and Ledder (1996), since the second term in this integrand is an equivalent expression for their result. It is also mentioned that c is the ratio between the hydraulic conductivity of the skin and the geometric mean of the vertical and horizontal hydraulic conductivities outside of the skin.

2.3. Drawdown solution outside the skin in an aquifer of infinite thickness

The drawdown solution outside of the skin s_2 is derived in Appendix B and given by

$$s_2(r, z) = \frac{-Qi}{4\pi^2 \Delta K_s r_w} \int_0^\infty W(\xi) K_0\left(\frac{r\xi}{a}\right) \times \sin(\xi z)\, d\xi, \qquad r_s < r < \infty, \qquad r_w > 0, \quad (15)$$

with

$$W(\xi) = \frac{J(\xi)}{K_0(r_s|\xi|/a)}[g(\xi) I_0(r_s\xi) + K_0(r_s\xi)]. \quad (16)$$

The function $g(\xi)$ and constant c are given by Eqs. (13) and (14), respectively. It is noted that s_2 is also an odd function in z, as expected from the geometry of the problem.

2.4. Drawdown solution in an aquifer of finite thickness

For a finite aquifer that has the two boundaries at $z = b_1$ and $z = b_2$, with $z = 0$ being the center of the two screened sections as in the infinite aquifer case, we can use the method of reflections to write down the

drawdown solution as the infinite series

$$s_F(r,z) = s_I(r,z) - s_I(r,z-2b_1) - s_I(r,z+2b_2) + s_I(r,z-(2b_1+2b_2)) + s_I(r,z+(2b_1+2b_2)) - s_I(r,z-(4b_1+2b_2)) - s_I(r,z+(2b_1+4b_2)) + s_I(r,z-(4b_1+4b_2)) + s_I(r,z+(4b_1+4b_2)) + \ldots \quad (17)$$

where s_I, is given by Eq. (10) for $r_w < r < r_s$ and Eq. (15) for $r > r_s$. Zlotnik and Ledder (1996) show that these series converge rapidly.

3. Average upper chamber drawdown

Field measurements in a well are obtained by taking a head measurement in the upper chamber. This measurable quantity can be represented by the average head over the screened section of the upper chamber. Define a function $S_u(y)$ by

$$S_u(y) = \frac{1}{2\Delta}\int_{L-\Delta}^{L+\Delta} s_1(r_w, z+y)\,dz. \quad (18)$$

From Eq. (10) we have

$$S_u(y) = \frac{-Q}{\pi^2\Delta^2 K_s r_w} \times \int_0^\infty \frac{\sin(\xi(L+y))\sin(\xi L)\sin^2(\xi\Delta)}{\xi^3} \times \frac{[g(\xi)I_0(r_w\xi) + K_0(r_w\xi)]}{[g(\xi)I_1(r_w\xi) - K_1(r_w\xi)]}\,d\xi, \quad (19)$$

where $g(\xi)$ and c are given by Eqs. (13) and (14), respectively. Note that the average head for an infinite aquifer is given by

$$S_{u,I} = S_u(0). \quad (20)$$

For an aquifer of finite thickness with boundaries at $z = b_1$ and $z = -b_2$, and with $z = 0$ being the center of the two screened sections, one integrates Eq. (17) from $(L-\Delta)$ to $(L+\Delta)$, with $r = r_w$, and divides by the chamber length 2Δ.

$$S_{u,F} = S_u(0) - S_u(-2b_1) - S_u(2b_2) + S_u(-2b_1-2b_2) + S_u(2b_1+2b_2) - S_u(-4b_1-2b_2) - S_u(2b_1+4b_2) + S_u(-4b_1-4b_2) + S_u(4b_1+4b_2) + \ldots \quad (21)$$

The drawdown in the lower chamber can be obtained by merely changing the sign on each term and changing the sign in each argument of $S_u(b)$ on the right-hand side of Eq. (21).

4. Streamlines

4.1. Stream function for an aquifer of infinite thickness

Streamlines provide a useful tool for the characterization of the flow. For axisymmetrical flow, Stokes' stream function (Bear, 1972) will be used to determine the streamlines. Differential equations for Stokes' stream function inside the skin and outside the skin will be given separately and then continuity is assumed at the skin–aquifer interface $r = r_s$.

Stokes' stream function is defined by

$$\frac{\partial\psi_1}{\partial r} = K_s r\frac{\partial s_1}{\partial z}, \quad (22)$$

and

$$\frac{\partial\psi_1}{\partial z} = -K_s r\frac{\partial s_1}{\partial r} \quad (23)$$

inside the skin and

$$\frac{\partial\psi_2}{\partial r} = K_z r\frac{\partial s_2}{\partial z}, \quad (24)$$

and

$$\frac{\partial\psi_2}{\partial z} = -K_r r\frac{\partial s_2}{\partial r} \quad (25)$$

outside the skin. To define ψ_1 uniquely, we also require

$$\psi_1(r_w, 0) = 0 \quad (26)$$

and for continuity at r_s, it is required that

$$\psi_2(r_s, 0) = \psi_1(r_s, 0). \quad (27)$$

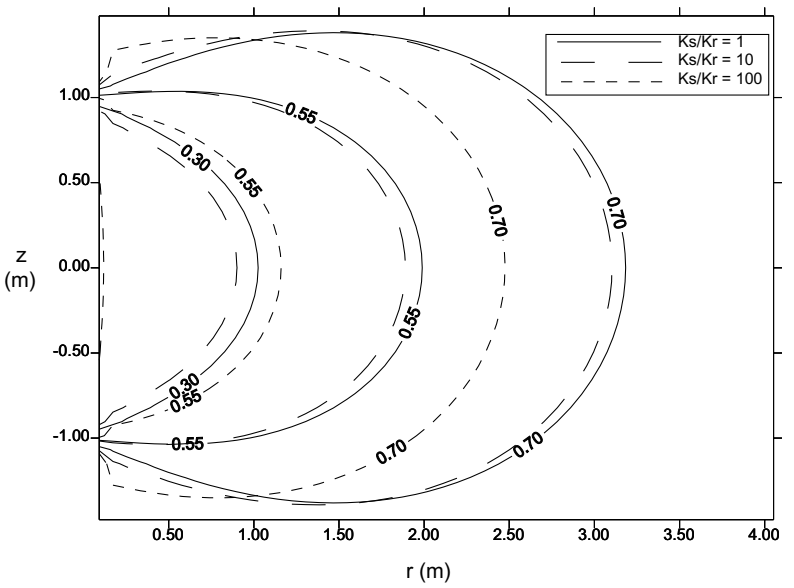

Fig. 2. Effects the skin conductivity has away from the well on the streamlines containing 30, 55 and 70% of the dipole flow in an infinite aquifer with $L = 1.0$ m, $\Delta = 0.1$ m, $r_w = 0.052$ m, $r_s = 0.104$ m, $a = 1.0$ and $K_s/K_r = 1, 10$, and 100.

Substituting Eq. (10) into Eq. (22) gives

$$\frac{\partial \psi_1}{\partial r} = \frac{-iQ}{4\pi^2 \Delta r_w} \int_0^\infty J(\xi)[g(\xi) r I_0(r\xi) + rK_0(r\xi)]\xi \cos(\xi z)\, d\xi,$$

which can be rewritten as

$$\frac{\partial \psi_1}{\partial r} = \frac{-iQ}{4\pi^2 \Delta r_w} \frac{\partial}{\partial r} \int_0^\infty J(\xi)[g(\xi) r I_1(r\xi) - rK_1(r\xi)] \cos(\xi z)\, d\xi, \quad (28)$$

and similarly,

$$\frac{\partial \psi_1}{\partial z} = \frac{-iQ}{4\pi^2 \Delta r_w} \frac{\partial}{\partial z} \int_0^\infty J(\xi)[g(\xi) r I_1(r\xi) - rK_1(r\xi)] \cos(\xi z)\, d\xi. \quad (29)$$

Comparing Eqs. (28) and (29):

$$\psi_1(r,z) = \frac{-iQ}{4\pi^2 \Delta r_w} \int_0^\infty J(\xi)[g(\xi) r I_1(r\xi) - rK_1(r\xi)] \cos(\xi z)\, d\xi + \text{const.}$$

The constant is $Q/2\pi$, from Eq. (26). Therefore, the stream function inside the skin, denoted by ψ_1, is given by

$$\psi_1(r,z) = \frac{Q}{2\pi} + \frac{-iQ}{4\pi^2 \Delta r_w} \int_0^\infty J(\xi)[g(\xi) r I_1(r\xi) - rK_1(r\xi)] \cos(\xi z)\, d\xi, \quad (30)$$

$$r_w < r < r_s,$$

where $J(\xi)$, $\hat{F}(\xi)$, $g(\xi)$, and c are given by Eqs. (11)–(14), respectively. Similarly, the stream function outside the skin is

$$\psi_2(r,z) = \frac{Q}{2\pi} + \frac{iQ}{4\pi^2 \Delta r_w c} \int_0^\infty W(\xi) r K_1\left(\frac{r\xi}{a}\right) \times \cos(\xi z)\, d\xi, \qquad r_s < r < \infty, \quad (31)$$

where $W(\xi)$, $\hat{F}(\xi)$, $g(\xi)$, and c are given by Eqs. (16), (12), (13) and (14), respectively.

4.2. The stream function for a finite aquifer

For a finite aquifer that has the boundaries at $z = b_1$ and $z = -b_2$, with $z = 0$ being the center of the two screened sections as in the infinite aquifer case, we can use the method of reflections again to write down

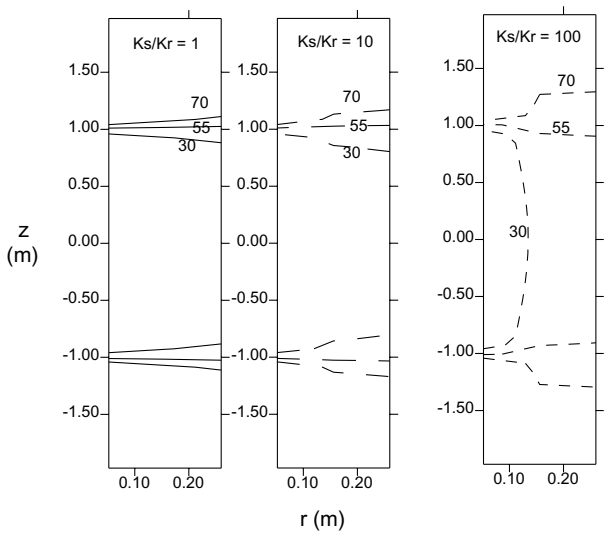

Fig. 3. Effects the skin conductivity has near the well on the streamlines containing 30, 55 and 70% of the dipole flow in an infinite aquifer with $L = 1.0$ m, $\Delta = 0.1$ m, $r_w = 0.052$ m, $r_s = 0.104$ m, $a = 1.0$ and $K_s/K_r = 1, 10,$ and 100.

the stream function as the infinite series

$$\psi_F(r,z) = \psi_I(r,z) - \psi_I(r,z-2b_1) - \psi_I(r,z+2b_2) + \psi_I(r,z-(2b_1+2b_2)) + \psi_I(r,z+(2b_1+2b_2)) - \psi_I(r,z-(4b_1+2b_2)) - \psi_I(r,z+(2b_1+4b_2)) + \psi_I(r,z-(4b_1+4b_2)) + \psi_I(r,z+(4b_1+4b_2)) + \ldots \quad (32)$$

where ψ_I is given by Eq. (30) for $r_w < r < r_s$ and Eq. (31) for $r > r_s$.

4.3. Normalized stream functions and streamlines

The equation for the entire domain around the well, including the skin in a finite or infinite aquifer is given by

$$\psi(r,z) = H(r_s - r)\psi_1(r,z) + H(r - r_s)\psi_2(r,z),$$

where H is the standard Heaviside function ($H(x) = 0,\ x < 0$; $H(x) = 1,\ x > 0$). ψ_1 is given by Eq. (30) and ψ_2 is given by Eq. (31) for the infinite aquifer case, and formula (32) is used for the finite aquifer case.

Following Zlotnik and Ledder (1996), the stream function is normalized by defining

$$\Psi(r,z) = \frac{\psi(r,z)}{\psi(\infty,0)} = \frac{2\pi\psi(r,z)}{Q}. \quad (33)$$

Therefore, streamlines range from 0.0 to 1.0 and are the surfaces generated by rotating the level curves given by

$$\Psi = \gamma \quad (34)$$

about the line $r = 0.0$. The fraction γ gives the percentage of the flow contained within this surface. Solving Eq. (34) for a given γ, one obtains the equation for that streamline. Figs. 2 and 3 display some examples where streamlines were computed as level curves of Ψ.

5. Analysis of the skin, anisotropy, well geometry and boundary effects

We discuss below the effect of the skin on the kinematic flow structure near the recirculation well. However, other factors, such as the anisotropy of hydraulic conductivity, well geometry and boundary effects can amplify or attenuate the effect of the skin. Finite-difference or finite-element analysis could be used for such studies, however, analytical expressions

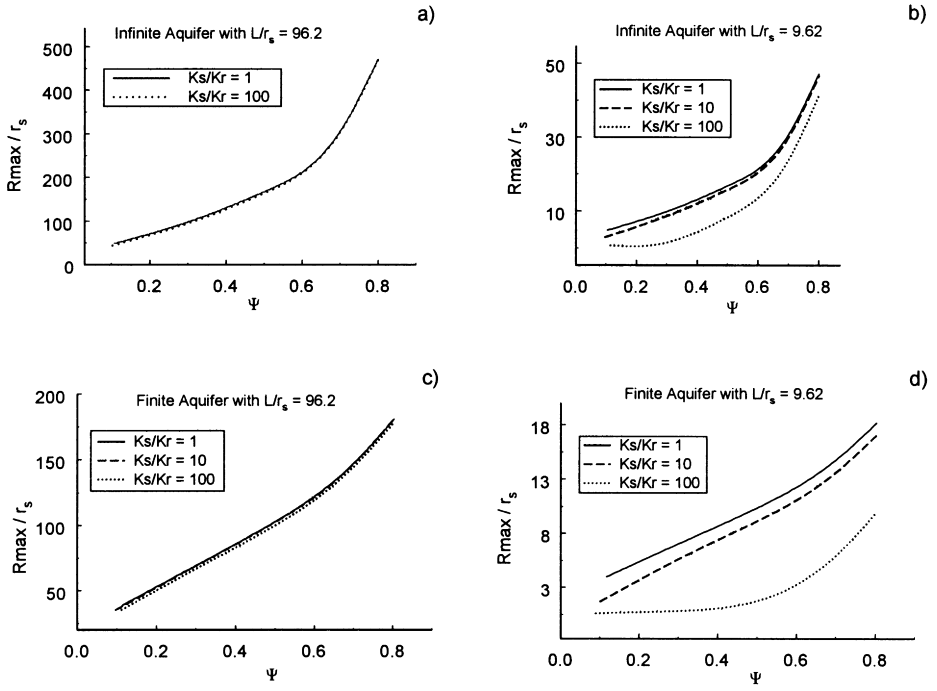

Fig. 4. Effects the skin conductivity has on the maximum radial extent of streamline R_{max} containing 10–80% of the dipole flow with $a = 1$, $r_w = 0.052$ m, $r_s = 0.104$ m in an infinite aquifer with (a) $L = 10.0$ m, $\Delta = 1.0$ m; (b) $L = 1.0$ m, $\Delta = 0.1$ m; and a finite aquifer having (c) $L = 10.0$ m, $\Delta = 1.0$ m, $b_1 = 11.0$ m, $b_2 = -11.0$ m; and (d) $L = 1.0$ m, $\Delta = 0.1$ m, $b_1 = 1.1$ m, $b_2 = -1.1$ m.

for Stokes' stream function are more direct and computationally efficient. The analysis is based on the results of numerous examples presented below.

5.1. Maximum radius of a streamline

Figs. 2 and 3 illustrate the effects of a skin layer on streamlines. When the hydraulic conductivity of the skin is greater than in the surrounding aquifer, $K_s/K_r > 1$, the streamlines are deformed. Presence of high hydraulic conductivities in the skin pull the streamlines closer to the well (Fig. 2). However, in the immediate vicinity of the recirculation well, the streamlines containing less than 55% of the flow ($\gamma \leq 0.55$) are pulled in, while the rest of the streamlines ($\gamma > 0.55$) spread out, away from the well due to the availability of a more permeable passage for the water within the skin (Fig. 3).

For remediation, it is important to know the extent to which a streamline has been pulled in due to the presence of the skin. Fig. 4(a)–(d) exhibits the maximum radial extent of a given streamline $\Psi = \gamma$ scaled by the distance r_s. For simplicity, an aquifer of infinite thickness is considered first and compared with a finite thickness aquifer later. Note that in an aquifer of infinite thickness, where the horizontal boundaries are far away from the upper and lower chambers, the maximum radial extent of a streamline occurs when the vertical coordinate is $z = 0$ due to the symmetry in the problem. For the finite aquifer analysis, we preserve this symmetry by placing the dipole in the center of the finite aquifer. Note also that $a = 1$ in all four parts of Fig. 4, so the case $K_s/K_r = 1$ gives a base line for the case without skin.

Fig. 4(a) illustrates that in an infinite aquifer an aspect ratio of $L/r_s = 96.2$, streamlines shift very little even in the extreme case when the skin–aquifer ratio is $K_s/K_r = 100$. Fig. 4(b) illustrates that in the same infinite aquifer, when we decrease the aspect ratio to $L/r_s = 9.62$, the skin is recognizable when the skin–aquifer ratio is $K_s/K_r = 10$ but is insignificant until $K_s/K_r = 100$.

In looking at a finite aquifer, the boundaries are assumed to be directly above the top screen and

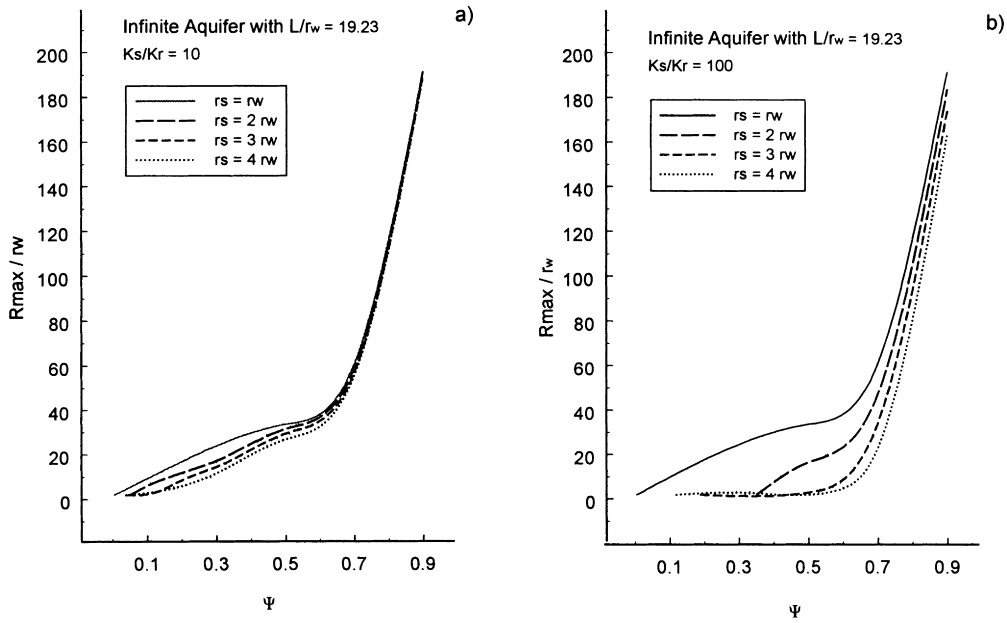

Fig. 5. Effects the radius of a skin layer has on the maximum radial extent of a streamline R_{max} containing 10–80% of the dipole flow with $a = 1$, $r_w = 0.052$ m, $L = 1.0$ m and $\Delta = 0.1$ m in an infinite aquifer with (a) $K_s/K_r = 10$, and (b) $K_s/K_r = 100$.

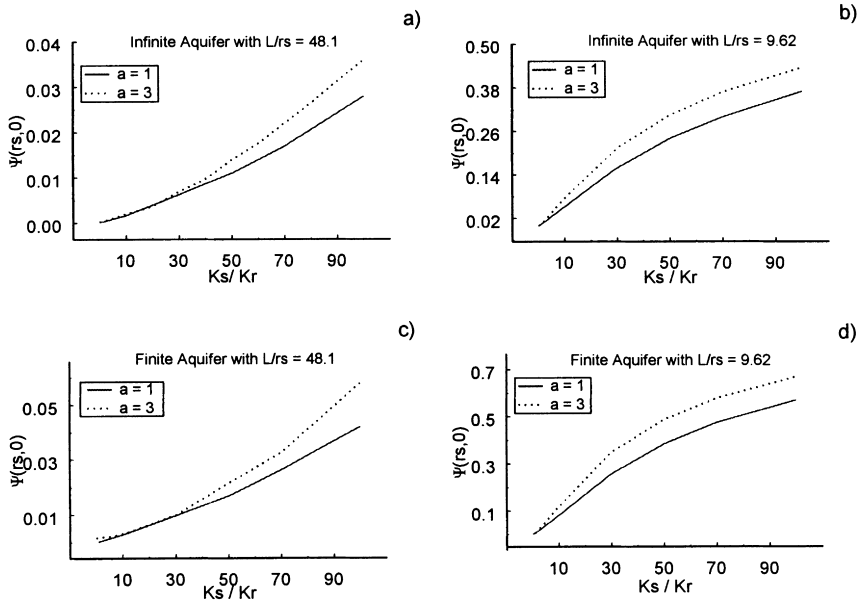

Fig. 6. Effects the skin conductivity has on the percentage of the dipole flow short-circuited through the skin layer vs the skin–aquifer conductivity ratio for different aquifer anisotropy ratios with $r_w = 0.052$ m and $r_s = 0.104$ m for aspect ratios in an infinite aquifer of (a) $L = 5.0$ m and $\Delta = 0.5$ m; (b) $L = 1.0$ m and $\Delta = 0.1$ m; and aspect ratios in a finite aquifer of (c) $L = 5.0$ m, $\Delta = 0.5$ m; and (d) $L = 1.0$ m, $\Delta = 0.1$ m.

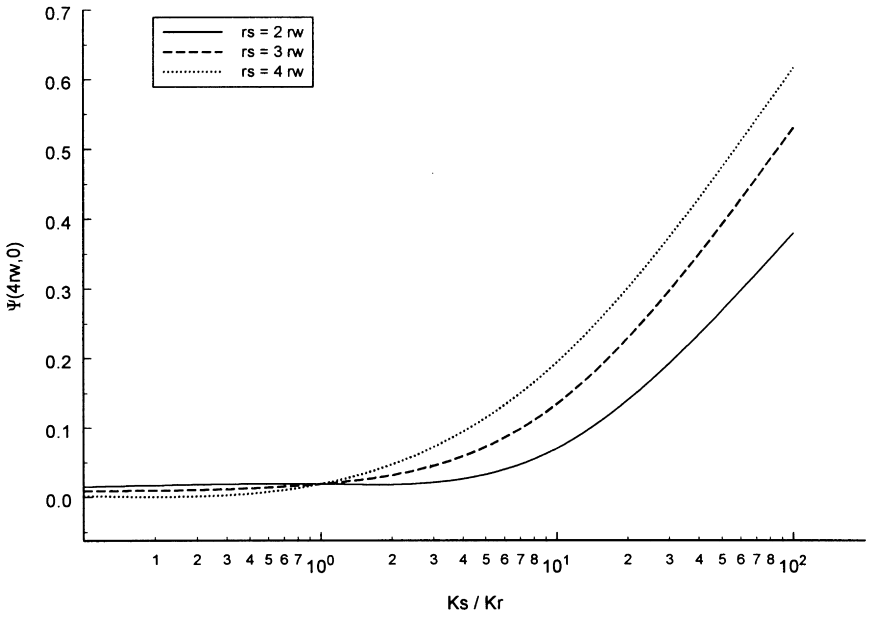

Fig. 7. Effects the radius and conductivity of the skin has on the percentage of the dipole flow contained within a radius of $4r_w$ with $r_w = 0.052$ m and $L = 1.0$ m and $\Delta = 0.1$ m in an infinite aquifer.

directly below the bottom screen ($-b_2 = -L - \Delta$, $b_1 = L + \Delta$). Fig. 4(c) illustrates that effects of the skin on the radial maximum extent of the streamline are still absent when the aspect ratio is $L/r_s = 96.2$, even in the presence of horizontal boundaries of a finite aquifer. By comparing Fig. 4(b) and (d), it is obvious that when the aspect ratio is $L/r_s = 9.62$, the presence of horizontal boundaries in a finite aquifer amplifies the effects of the skin layer. In a typical aquifer remediation, the screened chambers are placed near the aquifer boundaries. Since most aquifers will have a thickness that will create aspect ratios on the order of 100, the most likely scenario for actual field situations in aquifer remediation is that of Fig. 4(c).

The radius of a hole drilled to install a well may vary for different wells. Therefore, we look at the effects that varying the radius of the skin will have on the flow. Fig. 5(a) and (b) shows this effect in an infinite aquifer with the same aspect ratio as Fig. 4(b), $L/r_w = 19.23$, and the $r_s = r_w$ line showing the no-skin case. By looking at Fig. 5(a) and (b), we again see that the skin pulls the streamlines in. With the ratio $K_s/K_r = 10$, it is shown that a large skin with $r_s = 4r_w$ pulls in the streamlines containing less than 50% of the flow ($\gamma < 0.5$) by at most 40%. However, when the ratio is extreme, $K_s/K_r = 100$, streamlines $\gamma < 0.5$ can be pulled in by as much as 85% for the large skin of $r_s = 4r_w$. Fig. 5(b) shows that the result in increasing the skin radius from three to four times the well radius is not as significant as increasing the skin radius from one to two or two to three times the well radius.

In summary, the skin layer reduces the radial extent of the streamline and the volume within this streamline. Presence of impermeable horizontal boundaries as well as the radius of the skin will further amplify these skin effects. However, the effects are important only when the aspect ratio L/r_s is in the order of 10 or less.

5.2. Short-circuiting effect

The percentage of flow retained in the skin is given by the expression $\Psi(r_s, 0)$, where Ψ is given by Eq. (30). As mentioned above, increasing the skin–aquifer hydraulic conductivity ratio K_s/K_r pulls in streamlines, increasing the value of $\Psi(r_s, 0)$. Fig. 6(a)–(d) exhibits this behavior by showing the percentage of flow remaining inside the skin vs the skin–aquifer hydraulic conductivity ratio for two different anisotropy ratios. Note that the uniform isotropic aquifer

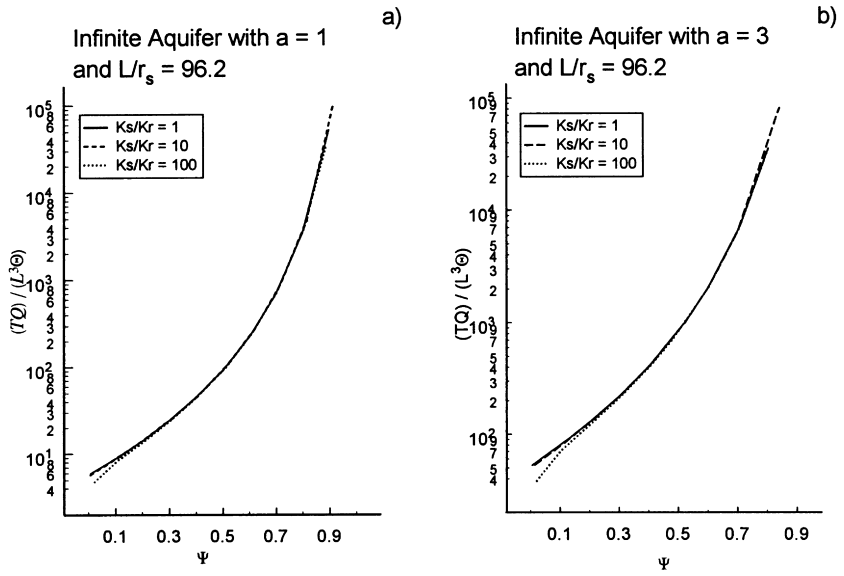

Fig. 8. Effects the conductive skin has on scaled travel times ($TQ/L^3\Theta$) for a water particle traveling on streamlines containing 10–90% of the dipole flow from the lower chamber to the upper chamber in an infinite aquifer with $L = 10.0$ m, $\Delta = 1.0$ m, $r_w = 0.052$ m, $r_s = 1.04$ m with anisotropy ratios of (a) $a = 1$; and (b) $a = 3$.

without skin ($a = K_s/K_r = 1$) gives a base line for the percentage of flow that stays within the skin layer. The skin thickness is taken to be twice the well radius: $r_s = 2r_w$.

Fig. 6(a) illustrates that even when K_s is 100 times larger than K_r in an infinite aquifer and an aspect ratio of $L/r_s = 48.1$, there is only a negligible amount of short-circuiting due to the effect of the skin. Fig. 6(b) shows that in an infinite aquifer and an aspect ratio of $L/r_s = 9.62$, the effects of the skin are amplified, with 10% of the flow lost through the skin for a modest skin–aquifer hydraulic conductivity ratio $K_s/K_r = 10$, and up to 40% of the flow can be lost through the skin when $K_s/K_r = 100$. In both cases of large and small chamber separations of the recirculation well, anisotropy ($a > 1$) increases the effect of the short-circuiting of groundwater flow due to a higher vertical resistance of the aquifer.

To estimate the effects of horizontal boundaries on the effect of short-circuiting in the finite aquifer, the horizontal boundaries are again placed directly above the top screen and directly below the bottom screen. Fig. 6(c) shows that horizontal boundaries only weakly enhance the short-circuiting when the aspect ratio is $L/r_s = 48.1$. By comparing Fig. 6(b) and (d), it is again clear that the presence of horizontal boundaries will enhance the effects of the skin more noticeably when the aspect ratio L/r_s is smaller.

In all the Fig. 6(a)–(d), it is noted that the skin effects are enhanced slightly when the anisotropy ratio is increased. However, the largest contributing factor in amplifying the effects of the skin is again with the aspect ratio L/r_s. This agrees with the intuition that the short-circuiting will be more pronounced when the two screened sections are closer together. As in the discussion of the maximum radius of a streamline, we observe that in the application of remediation, the influence of the skin is not significant due to large aspect ratios L/r_s typically encountered in the field.

Due to the continuous pumping, the skin may get plugged with fine clay particles and the skin conductivity can actually become lower than the surrounding region. Fig. 7 shows the value of the streamline that is a distance of $4r_w$ from the well as we vary the skin radius from no skin to $4r_w$ in an infinite aquifer with $L/r_w = 19.23$. It is seen that when the ratio $K_s/K_r < 1$, i.e. a lower conductive skin than the surrounding aquifer, that there is very little effect on the streamlines. However, for $K_s/K_r > 1$, the radius of skin will have a

noticeable effect on the streamlines as shown in Fig. 5. Note that when the ratio $K_s/K_r = 100$ and $r_s = 4r_w$, there is a 65% of the flow contained within the skin.

5.3. Travel times along streamlines

Since the effect of the skin has an effect on the lengths of the streamlines, it is intuitive that the skin will affect the travel times for a water particle to travel from one screen to another along a given streamline. The velocity vector **V** at each point is given by $V_r = (K_s/\theta)(\partial s/\partial r)$ and $V_z = (K_s/\theta)(\partial s/\partial z)$ inside the skin and $V_r = (K_r/\theta)(\partial s/\partial r)$ and $V_z = (K_z/\theta)(\partial s/\partial z)$ outside of the skin where θ is the aquifer porosity (which is assumed uniform within and outside the skin). Using a fourth order Runge–Kutta (e.g. Press et al., 1989) routine, one can track a water particle traveling a given streamline by solving the system $dr/dt = V_r$, $dz/t = V_z$. The initial conditions for this non-linear system of ordinary differential equations are $r(0) = r_0$ and $z(0) = z_0$, where (r_0, z_0) are coordinates of a point on the desired streamline.

All the analysis were performed for a well radius of $r_w = 0.05$ m. For a fixed initial radial position of $r_0 = 0.065$ m (to accelerate convergence in the calculations), an appropriate initial vertical coordinate z_0 was chosen to place the particle on the desired streamline for which we wanted to calculate travel times between screens. Since the travel times are only important in remediation applications, only the large aspect ratio L/r_s was investigated.

Fig. 8 displays the travel times that takes for a particle to travel from one screen to the other along streamlines containing different percentages of the flow, scaled by the time $\theta L^3/Q$. A comparison between Fig. 8(a) and (b) indicates once again that the skin effects are not noticed with the large aspect ratio $L/r_s = 96.2$ even with an increase in the anisotropy ratio. However, one important observation from Fig. 8(a) and (b) is that the travel times increase significantly (in the order of 10) for a modest increase in anisotropy ratio from $a = 1$ to $a = 3$ for streamlines containing less than half of the flow ($\Psi < 0.5$). This is where the most intensive water exchange between the two chambers occurs. This is intuitive, as flow is more horizontal as an increase due to a vertical "resistance" of the aquifer, and thus the paths are longer. Note that in the absence of skin, the factor a can be absorbed into the scale for r. This means that doubling a doubles the radial distance covered by a streamline. Fig. 2 only considers the effect of skin for fixed a, so it provides no intuition about the effects of a.

5.4. Flushed volume of the aquifer

Another important consideration for aquifer remediation using vertical circulation wells is the flushed volume of the aquifer. Consider the example of an infinite aquifer with $L = 10.0$, $\Delta = 1.0$, $r_w = 0.052$, $r_s = 0.104$ m, and $a = K_s/K_r = 1.0$. If we rotate the streamline containing 60% of the flow about the $r = 0.0$ axis and consider an aquifer porosity of $\theta = 0.2$, the volume of water contained in this region is obtained by a simple numerical integration scheme using shells. The volume of water for this scenario is 5772 m^3. Considering a pumping rate of $Q = 30.0$ m^3/day, this volume of water is pumped in 192.4 days. However, the actual travel time along the 60% streamline with this geometry is approximately 1500 days. Therefore, the flushed volume and the pumping volume $V = Qt$ differ significantly. While it takes 1500 days to travel the streamline containing 60% of the flow, the other streamlines contained in this region have shorter travel times. As an example, the 20% streamline for this geometry has a travel time of around 100 days. Therefore, the region surrounding the 20% streamline is flushed 15 times in the time that the region surrounding the 60% streamline will be flushed once.

6. Summary

In this study, analytical solutions for the drawdown and streamlines were derived for the case of a vertical circulation well in an aquifer with no ambient flow. The analysis included the effects of a disturbed zone (skin) surrounding the well, and modeled the well as a combination of a source and sink that are uniformly distributed over the cylindrical screened sections. The skin layer was assumed to be isotropic and uniform, but differing in properties from the undisturbed aquifer, which was considered to be uniform, but not necessarily isotropic. Examples included the basic model of an aquifer with no horizontal boundaries

and also a confined aquifer with two impermeable horizontal boundaries.

The presence of skin which is less resistant to flow than the undisturbed material tends to deform streamlines radially inward. A skin with higher conductivity than the ambient aquifer tends to create short-circuiting, whereby a portion of flow moves from one chamber to the other without ever entering the undisturbed aquifer at all. These effects are diminished by increasing the distance between the chamber centers. For the typical remediation case, in which the chambers extend almost to the horizontal boundaries of the aquifer, the chamber center separation is large enough that the effect of the skin is minimal, even when the conductivity of the skin is two orders of magnitude greater than that of the surrounding aquifer. We may conclude that the skin can safely be ignored in such cases. The presence of horizontal impermeable boundaries has the effect of reducing the radial extent of each given streamline.

An additional effect was demonstrated by the model, regardless of whether or not the skin is considered. Travel times along a streamline were shown to vary greatly as different streamlines are considered. Thus, the region near the well is flushed many times by the flow in the time it takes the region in the middle of the flow zone to be flushed once. The design of a remediation system necessarily includes, decisions about the spacing of wells and the length of time the system runs. There is clearly a trade-off between these design features. If the system is to be run only a short time, then only the inner region of the flow will be completely flushed, so the wells will have to be close together. If the wells are spaced so that their flow zones overlap only slightly, then the system will have to be operated for a very long time in order to completely flush the whole region.

Acknowledgements

This work was partially supported by grants from the National Water Research Institute, the US Geological Survey, and the Water Center of the University of Nebraska—Lincoln. The authors of this paper would like to thank the referees for their comments and suggestions.

Appendix A. Derivation of Eq. (10)

The differential Eqs. (1) and (2) can be written collectively as

$$a_i^2 \frac{1}{r}\frac{\partial}{\partial r}\left(r\frac{\partial s_i}{\partial r}\right) + \frac{\partial^2 s_i}{\partial z^2} = 0, \qquad i = 1, 2, \tag{A1}$$

where $a_1^2 = 1$ and $a_2^2 = K_r/K_z = a^2$. The Fourier transform of s_i is defined by

$$\hat{s}_i = \int_{-\infty}^{\infty} s_i(r, z)\, e^{i\xi z}\, dz. \tag{A2}$$

In the transform domain, Eq. (A1) becomes

$$r^2\hat{s}'' + r\hat{s}' - \frac{|\xi|^2 r^2 \hat{s}}{a_i^2} = 0, \tag{A3}$$

where the prime notation refers to differentiation in r. Therefore,

$$\hat{s}_1(r, \xi) = A(\xi)I_0(r|\xi|) + B(\xi)K_0(r|\xi|) \tag{A4}$$

and

$$\hat{s}_2(r, \xi) = C(\xi)K_0(r|\xi|/a) + D(\xi)I_0(r|\xi|/a), \tag{A5}$$

where I_0 and K_0 are the modified Bessel functions.

Since $I_0(r|\xi|/a) \to \infty$ as $r \to \infty$ and $K_0(r|\xi|/a) \to 0$ as $r \to \infty$, we have $D(\xi) = 0$ from Eq. (A5). Therefore,

$$\hat{s}_2(r, \xi) = C(\xi)K_0(r|\xi|/a). \tag{A6}$$

The continuity condition (A6) gives

$$A(\xi)I_0(r_s|\xi|) + B(\xi)K_0(r_s|\xi|) = C(\xi)K_0(r_s|\xi|/a). \tag{A7}$$

Condition (A7), along with the property that $(\partial/\partial r)I_0(r) = I_i(r)$ and $(\partial/\partial r)K_0(r) = -K_1(r)$, gives

$$K_s A(\xi)I_1(r_s|\xi|) - K_s B(\xi)K_1(r_s|\xi|) = -\frac{K_r}{a}C(\xi)K_1(r_s|\xi|/a). \tag{A8}$$

Eliminating $C(\xi)$ from these two equations, we get

$$A(\xi)\frac{I_0(r_s|\xi|)}{K_0(r_s|\xi|/a)} + B(\xi)\frac{K_0(r_s|\xi|)}{K_0(r_s|\xi|/a)} = -\frac{K_s a}{K_r}A(\xi)\frac{I_1(r_s|\xi|)}{K_1(r_s|\xi|/a)} + \frac{K_s a}{K_r}B(\xi)\frac{K_1(r_s|\xi|)}{K_1(r_s|\xi|/a)}. \tag{A9}$$

Let

$$c = \frac{K_s a}{K_r} = \frac{K_s}{\sqrt{K_r K_z}}. \tag{14}$$

Then,

$$A(\xi) = B(\xi) g(\xi) \tag{A10}$$

where

$$g(\xi) = \frac{c(K_1(r_s|\xi|)K_0(r_s|\xi|/a) - K_0(r_s|\xi|)K_1(r_s|\xi|/a)}{cI_1(r_s|\xi|)K_0(r_s|\xi|/a) + I_0(r_s|\xi|)K_1(r_s|\xi|/a)}. \tag{13}$$

The transformed drawdown is now known for the skin region, with the exception of the single unknown function B(ξ):

$$\hat{s}_1(r,\xi) = B(\xi)[g(\xi)I_0(r|\xi|) + K_0(r|\xi|], \quad r_w < r < r_s. \tag{A11}$$

Applying the Fourier transform to Eq. (3) gives

$$\lim_{r \to r_w} r \frac{\partial \hat{s}_1}{\partial r}(r,\xi) = \frac{Q\hat{F}(\xi)}{4\pi\Delta K_s},$$

where $\hat{F}(\xi)$ is given by

$$\hat{F}(\xi) = \frac{4i \sin(\xi L) \sin(\xi\Delta)}{\xi}. \tag{12}$$

Substituting Eq. (A1) into this limit yields

$$B(\xi) = \frac{QJ(\xi)}{4\pi\Delta K_s r_w}, \tag{A12}$$

where

$$J(\xi) = \frac{\hat{F}(\xi)}{|\xi|[g(\xi)I_1(r_w\xi) - K_1(r_w\xi)]} \tag{11}$$

was introduced to simplify the notation. The transformed drawdown inside the skin region is then given by

$$\hat{s}_1(r,\xi) = \frac{QJ(\xi)}{4\pi\Delta K_s r_w}[g(\xi)I_0(r|\xi|) + K_0(r|\xi|)], \tag{A13}$$

$r_w < r < r_s$.

Using the inversion formula, we get

$$s_1(r,z) = \frac{-iQ}{4\pi^2\Delta K_s r_w}\int_0^\infty J(\xi)[g(\xi)I_0(r\xi) + K_0(r\xi)]\sin(\xi z)\,d\xi, \tag{10}$$

$r_w < r < r_s$.

Appendix B. Derivation of Eq. (15)

The drawdown solution outside of the skin is known in the transform domain (A6) with the unknown function $C(\xi)$ yet to be determined. Eqs. (6), (A11) and (A12) are used to determine

$$C(\xi) = \frac{QJ(\xi)}{4\pi\Delta K_s r_w K_0(r_s|\xi|/a)}[g(\xi)I_0(r_s|\xi|) + K_0(r_s|\xi|)]. \tag{B1}$$

To simplify the notation, let

$$W(\xi) = \frac{J(\xi)}{K_0(r_s|\xi|/a)}[g(\xi)I_0(r_s\xi) + K_0(r_s\xi)]. \tag{16}$$

From Eqs. (A6), (B1), (11) and (13), the transformed drawdown solution outside of the skin $\hat{s}_2$ is again an odd function in ξ, and will therefore be written as a sine transform upon inversion,

$$s_2(r,z) = \frac{-Qi}{4\pi^2\Delta K_s r_w}\int_0^\infty W(\xi)K_0\left(\frac{r\xi}{a}\right) \times \sin(\xi z)\,d\xi, \qquad r_s < r < \infty, \qquad r_w > 0, \tag{15}$$

with $W(\xi)$, $J(\xi)$, $g(\xi)$, and c given by Eqs. (16), (11), (13) and (14), respectively.

References

Bear, J., 1972. Dynamics of Fluids in Porous Media, Elsevier, New York.

Gvirtzman, H., Gorelick, S.M., 1992. The concept of in situ vapor stripping for removing VOCs from groundwater. Transport Porous Media 8, 71–92.

Gvirtzman, H., Gorelick, S.M., 1993. Using air-lift pumping as an in situ aquifer remediation technique. Water Sci. Technol. 27 (7–8), 195–201.

Herrling, B., Buermann, W., 1990. A new method for in-situ remediation of volatile contaminants in groundwater-numerical simulations of the flow regime. In: Gambolati, G., Rinaldo, A., Brebbia, C., Gray, W., Pinder, G. (Eds.). Computational

Methods in Subsurface Hydrology VIII, Springer, Berlin, pp. 299–304.

Herrling, B., Stamm, J., 1992. Numerical results of calculated 3D vertical circulation flows around wells with two screen sections for in-situ on-site aquifer remediation. In: Russel, T.F., Ewing, R.E., Brebbia, C.A., Gray, W., Pinder, G. (Eds.). Computational Methods in Water Resources IX, Numerical Methods in Water Resources, 1. Elsevier Applied Science, New York, pp. 483–492.

Herrling, B., Stamm, J., Buerman, W., 1991. Hydraulic circulation systems for in-situ bioreclamation and/or in-situ remedies of strippable contamination. In: Hinchie, R.E., Olfenbuttel, R.F. (Eds.). In-situ Bioreclamation: Applications and Investigations for Hydrocarbon and Contaminated Site Remediation, Butterworth-Heinemann, Stoneham, MA, pp. 173–195.

Indelman, P., Zlotnik, V., 1997. Average steady non-uniform flow in stratified formations. Water Resour. Res. 33 (5), 927–934.

Kabala, Z.J., 1993. Dipole flow test: a new single-borehole test for aquifer charaterization. Water Resour. Res. 29 (1), 99–107.

Kabala, Z.J., Xiang, J., 1992. Skin effect and its elimination for single borehole aquifer tests. In: Russel, T.F., Ewing, R.E., Brebbia, C.A., Gray, W., Pinder, G. (Eds.). Computational Methods in Water Resources IX, Numerical Methods in Water Resources, I. Elsevier Applied Science, New York, pp. 467–474.

Press, W.M., Flannery, B.P., Teukolsky, S.A., Vetterling, W.T., 1989. Numerical Recipes (Fortran Version), Cambridge University Press, Cambridge, MA.

Van Peursem, D., Ledder, G., Zlotnik, V., 1998. The kinematic flow structure for the Gvirtzman–Gorelick in situ VOC remediation system. Transport Porous Media 30, 363–376.

Zlotnik, V., Ledder, G., 1994. Effect of boundary conditions on dipole flow. In: Peters, A. et al. (Eds.). Computational Methods in Water Resources X, 2. Kluwer Academic, Dordrecht, Netherlands, pp. 907–914.

Zlotnik, V., Ledder, G., 1996. Theory of flow in uniform anisotropic aquifers. Water Resour. Res. 32 (4), 1119–1128.

Zlotnik, V.A., Zurbuchen, B.R., 1998. Dipole probe: design and field applications of a single-borehole device for measurements of vertical variations of hydraulic conductivity. Ground Water 36 (6), 884–893.